RESEARCH ARTICLE

Soil moisture derivation using triangle method in the lighvan watershed, north western Iran

M. Rahmati*, M.M. Oskouei[2], M.R. Neyshabouri[3], J.P. Walker[4], A. Fakherifard[5], A. Ahmadi[3], S.B. Mousavi[1]

[1] *University of Maragheh, Faculty of Agriculture, Department of Soil Science, Maragheh, Iran.*Corresponding autor: mehdirmti@gmail.com [2] Sahand University of Technology, Mining Engineering Faculty, Tabriz, Iran.* [3] *University of Tabriz, Faculty of Agriculture, Department of Soil Science, Tabriz, Iran.* [4] *Monash University, Faculty of Engineering, Department of Civil Engineering, Melbourne, Australia.* [5] *University of Tabriz, Faculty of Agriculture, Department of Water Engineering, Tabriz, Iran.*

Abstract

Soil moisture determination plays a major role in water and crop management. In this research, the accuracy of the Triangle Method (*TM*) was evaluated to predict surface soil moisture content using Moderate Resolution Imaging Spectro-radiometer (*MODIS*) satellite images with 1km resolution. The investigation was carried out within an area of 76 km^2 in Lighavn watershed in East Azerbaijan, North West of Iran. The analysis was based on ground measurements of soil moisture at 225 points (45 pixels) across the catchment on 2 different days. Ground measurements from the first day were used to train the models, while those from the second day were used for validation. A range of polynomial regressions from 1st to 4th orders were established between the ground measured soil moisture and *MODIS* Normalized Difference Vegetation Index (*NDVI*) and Land Surface Temperature (*LST*). The best results were obtained for the 4th order polynomial of the *TM* with the efficiency error (*ER*) and adjusted determination coefficient (R^2_{adj}) criterions, respectively, equal to 11.0% and 0.63 for calibration and 15.9% and 0.60 for validation stage. Therefore, the *TM* was found to provide reliable estimates of soil moisture, without the need for prior information of the soil surface roughness or the vegetation type and water content.

Keywords: Soil moisture, *NDVI*, land surface temperature, moisture monitoring

1. Introduction

Soil moisture is an important parameter for the Soil Water Balance Equation (*SWBE*) at global, regional, and local scales, including quantification of its components (infiltration, surface runoff, evapotranspiration, and deep percolation), and exchanges in the vadose zone (Davenport *et al.* 2005). Soil moisture is often referred to as surface soil moisture, meaning the water in upper 10 cm layer, or root zone soil moisture, meaning the water in the upper 100 to 200 cm of soil (Wang and Qu 2009). Importantly, soil moisture affects human health and plays an important role in agriculture, economic,

military, and transportation activities (Serrano 2010). Therefore, sustainable agriculture and water resource management need accurate information of the surface soil moisture. For example, low soil moisture for sustained periods results in drought and plant water deficit, potentially leading to wild fire (Serrano 2010). Conversely, high soil moisture leads to increased risk of flood. Moreover, evaporation rate which is strongly correlated to soil moisture makes a strong connection between land surface and atmosphere (Guo *et al.* 2005). Therefore, information about the spatial patterns of soil moisture at regional scale can helps to predict storms, the occurrence of frosts and heat waves, and the likelihood of limited vision due to thick fog (Serrano 2010). In addition to traffic-ability of tanks and visibility for jets, soil moisture is important for range of other military applications, e.g. the calculation of density altitude for determining the lift capacity of aircraft[1].

Direct observations of soil moisture are currently limited to measurements at specific locations. Moreover, such point-based measurements do not represent the spatial distribution of soil moisture, since it is highly variable both spatially and temporally (Engman 1991; Wood *et al.* 1992). However, technological advances in satellite remote sensing have offered a variety of approaches (Shi *et al.* 1997, Wen *et al.* 2003; Das *et al.* 2008; Van doninck *et al.* 2011) for measuring soil moisture across a wide area continuously over time. Empirical approaches construct functional relationships between measured variables, while the theoretical ones apply complicated scattering phenomena from probabilistic models of soil, vegetation, and terrain (Ahmad *et al.* 2010). Remote sensing, consequently, provides an opportunity for routine monitoring of soil moisture

across large scales (Wang and Qu, 2009) as well as vegetation moisture content (Castro *et al.* 2014).

Wang and Qu (2009) have classified techniques for the remote sensing of the near-surface soil moisture into 1. visible, 2. thermal infrared, and 3. microwave techniques. Microwave techniques, including radiometer (passive) and radar (active), are currently the preferred approaches for soil moisture remote sensing due to their all-weather capability and stronger relationship with the soil water content. While the more easily interpreted radiometer data is coarse and needs to be downscaled to be used for many of the applications discussed above, the radar data are infrequent through time and are very difficult to interpret, primarily due to need of ancillary surface roughness and vegetation information (Wang and Qu 2009). Although visible and thermal infrared are affected by clouds, they have fine spatial resolution and can be easier to interpret than radar (Wang and Qu 2009).

The thermal emission has a wavelength region between 3.5 and 14 μm (Curran 1985). Remote sensing of the surface soil moisture using optical data relies on either the use of thermal observations alone (Schmugge 1978; Friedl and Davis 1994), or in combination with vegetation indices (Chauhan *et al.* 2003). The Triangle Method (*TM*) is categorized as a thermal infrared technique (Wang and Qu 2009), and uses both Land Surface Temperature (*LST*) and the Normalized Difference Vegetation Index (*NDVI*) for remote sensing of the surface soil moisture using the Moderate Resolution Imaging Spectro-radiometer (*MODIS*) satellite images with 1 km resolution data.

The *TM* was first introduced by Price (1990) and then elaborated upon by others (Carlson *et al.* 1994; Carlson *et al.* 1995; Gillies and Carlson 1995; Lambin and Ehrlich 1996; Gillies *et al.* 1997; Owen *et al.* 1998; Jiang and Islam 1999, 2001, 2003; Chauhan

et al. 2003). The *TM* method has been verified by different investigations (Gillies *et al.* 1997; Carlson 2007; Wang *et al.* 2007; Mekonnen 2009) showing a good performance (with R^2 varying between 0.6 and 1.0) to predict soil moisture.

Due to the encouraging results of the recent studies, this paper explores the use of the *TM* method using 1km resolution *MODIS* data for the unique soil, vegetation, and weather conditions in North Western Iran.

2. Theoretical background of the method

The triangle method (Chauhan *et al.* 2003) is classified as a thermal infrared technique for soil moisture estimation using remotely sensed data (Wang and Qu 2009). It is a stepwise algorithm that is performed according to: 1. ground measurement of the soil moisture, 2. computation of the *NDVI* and *LST* from satellite images, 3. scaling the computed *NDVI* and *LST* to *NDVI** and *LST**, 4. constructing polynomials between the measured soil moisture and *NDVI** and *LST**, and 5. mapping the soil moisture using the derived equations. The *NDVI** and *LST** are computed according to: $\qquad$ (1) (2)

$$NDVI^* = \frac{NDVI - NDVI_{min}}{NDVI_{max} - NDVI_{min}}$$

$$LST^* = \frac{LST - LST_{min}}{LST_{max} - LST_{min}}$$

where *NDVI* and *LST* are the observed values for each pixel, and subscripts max and min imply the maximum and minimum values, respectively. The min and max for the parameters were set to be minimum and maximum for the particular pixel

over the season. Carlson *et al.* (1994) showed that the relationship among soil moisture (*M*), *NDVI**, and *LST** is expressed through a regression formula such as:

$$M = \sum_{i=0}^{i=n} \sum_{j=0}^{j=n} a_{ij} NDVI^{*(i)} T^{*(j)} \qquad (3)$$

where a_{ij} is the regression coefficient and the superscripts *i* and *j* imply the degree of the polynomials that are chosen for the regression.

3. Methods and Materials

3.1. Study area

The study was conducted in the Lighvan watershed, East Azerbaijan, located in North Western Iran (Figure 1). The watershed is located at the Sahand Mountain with latitude 37° 43' 07" to 37° 50' 08" N and longitude 46° 22' 23" to 46° 28' 05" E. The Lighvan watershed has an area of 7,854 hectares and an elevation varying from 3,534m in the uplands to 2,190m at the watershed outlet (Figure 2), with an average precipitation of 320 mm per year. Nearly all parts of the study area have coarse textured soils at soil surface (0-10 cm) consisting of loam, sand, sandy clay loam, sandy loam, and silt loam texture classes (Figure 3-A) (Rahmati, 2014). The major part of the study area consists of bare land (46%) and poor pasture (42%) land-uses (Figure 3-B) (Rahmati, 2014). Irrigated and dry-land farming covers only 12% of the area (Rahmati, 2014).

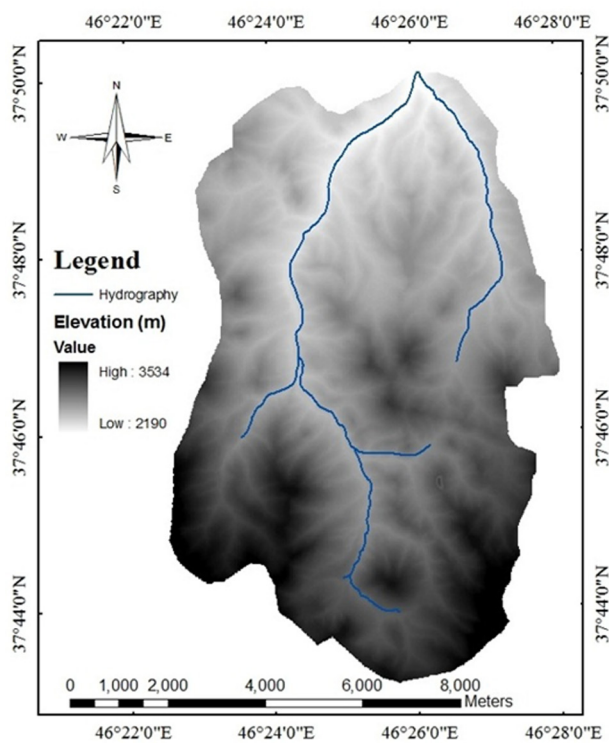**Figure 1.** Location of the study area in East Azerbaijan, Iran

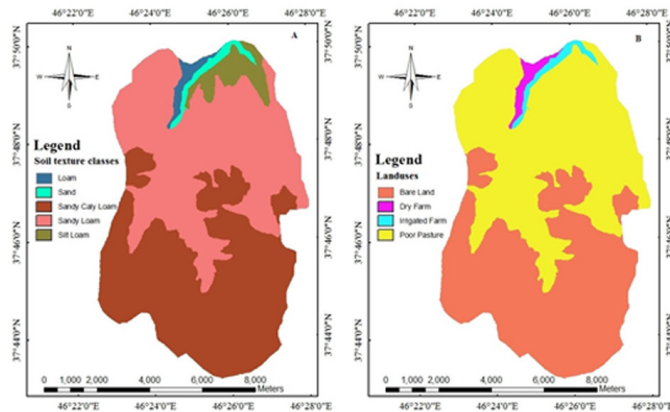**Figure 2**. DEM and river network map of the study area

Figure 3. Soil (A) and landuse (B) maps of the study area

3.2. Field and laboratory experiments

For sampling purposes, the study area was divided into 1 square kilometer pixels (the same as the *MODIS* resolution), and soil samples were collected from the 0 to 15 cm surface layer in each pixel. In total, 225 soil samples were taken from 45 out of 60 complete pixels for volumetric soil moisture determination. In other words, five samples were collected for each pixel and a simple mean was used to combine samples to produce an estimate for each pixel. Figure 4 indicates the location of the sampled pixels and the sampling strategy for each pixel. The Sampling was randomly repeated in two different days (11-June-2012 and 18-June-2012) with the first day's data used to calibrate the polynomials and the second day's data for validation. No rainfall occurred during the period 11-June till 18-June 2012.
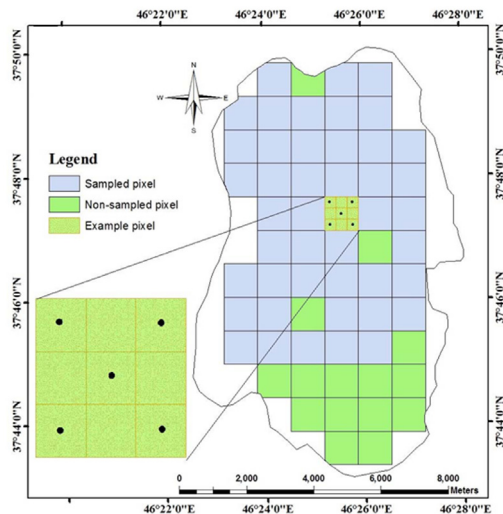

Figure 4. Location of the sampled cells and distribution of sampling points in the study area

The *MODIS* sensor is located on the *Aqua* and *Terra* satellites, having both day and night overpasses. Aqua and Terra products of *MODIS* were downloaded from the *MODIS* Adaptive Processing System (*MODAPS*) through Level 3 and Atmosphere Archive and Distribution System (*LAADS*) at http://ladsweb.nascom.nasa.gov. *MODIS/Terra* and its official *LST* (*MOD11A1*) and *NDVI* (*MOD13A2*) products were selected for analysis in this investigation, due to being less cloud affected than *Aqua* (Mekonnen 2009).

Although, the *MODIS* data of the study area on 11-Jun-2012 and 18-Jun-2012 were needed to fulfill this research, the data acquired on 9-Jun-2012 and 15-Jun-2012, respectively, were used due to being cloud free. There was no rainfall between days 9 to 11 and 15 to 18 of Jun-2012 to affect soil moisture content significantly.

3.3. Training and evaluation of the models

In this research, the 1st to 4th order polynomials were calibrated for their predictive skill in estimating soil moisture by the *TM* method, using *MODIS* images as input. The ground measurement of soil moisture was carried out on two different days, being the 11th and 18th June 2012. The measured data on 11th June were used to calibrate polynomials, while data on 18th June 2012 were used for validation. The *MODIS NDVI* and *LST* products of days 9th and 15th June 2012 were used instead of 11th and 18th June 2012, respectively, since the obtained data of 11th and 18th June 2012 were cloud affected. In this case, we assumed that the measured soil moisture on 11th June was correspond for 9th June and those measured on 18th June was correspond for 15th June due to inconsiderable change in soil moisture during one or two days.

3.4. Terrain correction

To check terrain effects due to the large elevation difference (around 1200 m) from the uplands to the outlet of the catchment, potential temperature (*T*) was required for elevation correction against *LST*. Potential temperature is the temperature that a parcel would acquire if adiabatically brought to standard reference pressure P_0, usually 1013mb (Mekonnen 2009). Potential temperature can be calculated according to (Mekonnen 2009):

$$T = LST \left(\frac{P_0}{P} \right)^{0.286} \tag{4}$$

where *T* is the potential temperature in K, *LST* is the land surface temperature in K, P_0 is the standard reference pressure usually 1013 mb, and *P* is the atmospheric pressure at the surface in mb, computed according to elevation (*Z*) by:

$$P = 1013 \left(\frac{293 - 0.0065Z}{293} \right)^{5.26} \tag{5}$$

where *Z* (km) was derived from resampling of the 30m resolution *DEM* into the 1km *MODIS* resolution using nearest neighbor resampling method. The computed value of T was then scaled using:

$$T^* = \frac{T - T_{min}}{T_{max} - T_{min}} \tag{6}$$

where *T* is the observed value for each pixel, while subscripts max and min imply the maximum and minimum values, respectively. Finally, polynomials were reconstructed between measured soil moisture and the *NDVI** and *T** information extracted form *MODIS* data to check elevation effects on polynomials evaluation.

3.5.Performance evaluation

Determination coefficient (R^2), adjusted determination coefficient (R^2_{adj}), Root Mean Square Error (*RMSE*), and evaluating error (*ER*) criterions were used to evaluate the accuracy of the method for soil moisture prediction. The *RMSE* and *ER* criterions were determined by using following equations:

$$RMSE=\sqrt{\frac{\sum_{i=1}^{N}\left[M_{i,Obs}-M_{i,Sim}\right]^2}{N}} \tag{7}$$

$$ER=\frac{RMSE}{M_{Obs}}\times100 \tag{8}$$

where $M_{i,Sim}$ and $M_{i,Obs}$ are the simulated and measured soil moisture at point i, M_{Obs} is the mean of measured soil moisture, and N is the number of measurements.

4. Results and Discussion

Statistics of the ground measured soil moistures for two sampling days are reported in Table 1. There was no rainfall event between two sampling days, with and approximately 0.02 cm³cm⁻³ decrease in soil moisture accordingly. The *NDVI* and *LST* maps of the study area on 9th June are depicted in Figure 5 and their statistical parameters for both sampling days reported in Table 1. According to the Table 1, the day time average of the LST for 9th and 15th June 2012 were 288.11 and 277.63K, respectively. Table 1 also reports that the average *NDVI* for sampling days were 0.254.
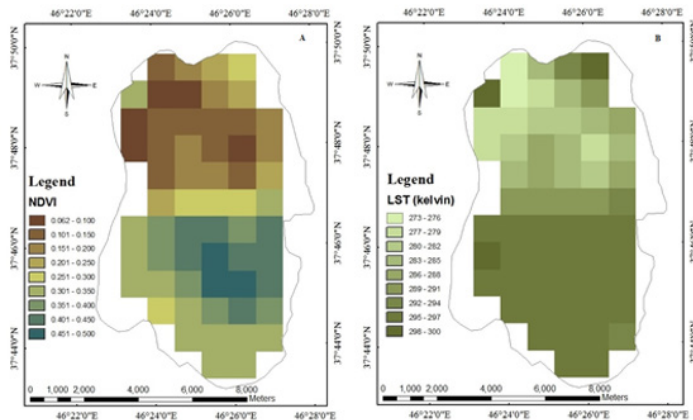

Figure 5. The NDVI (A) and LST (B) maps of the study area on 9-Jun-2012

Table 1. Statistics of ground measured soil moisture (M), and MODIS LST and NDVI of the study area

Parameter	9-Jun-2012			15-Jun-2012		
	M (cm³/cm³)	LST (°K)	NDVI	M (cm³/cm³)	LST (°K)	NDVI
Min	0.124	272.66	0.062	0.100	275.15	0.062
Max	0.263	299.68	0.473	0.237	284.35	0.473
Mean	0.169	288.11	0.254	0.150	277.63	0.254
Standard deviation	0.031	7.526	0.130	0.30	2.325	0.130

4.2. Polynomials training and evaluating

The Data Solver application of the Microsoft Office Excel was used to calibrate the polynomials. The following equation shows the expanded form of Equation. (3) for the 4th order polynomial used in this study:

$$M = \sum_{i=0}^{i=4} \sum_{j=0}^{j=4} a_{ij} \, NDVI^{*(i)} \, LST^{*(j)} = a_{00} NDVI^{*(0)} \, LST^{*(0)} + a_{01} NDVI^{*(0)} \, LST^{*(1)} + \qquad (9)$$

$$... + a_{43} NDVI^{*(4)} LST^{*(3)} + a_{44} NDVI^{*(4)} LST^{*(4)}$$

The results of polynomial evaluation for both calibration and validation stages are listed in Table 2. The outcome showed that an increase in the order of polynomials has resulted in a better prediction of the soil moisture. The 4th and 1st order polynomials possess the highest ($RMSE$=0.019 cm³cm⁻³, ER=11%, and R^2_{adj}=0.63) and lowest ($RMSE$=0.022 cm³cm⁻³, ER=13%, and R^2_{adj}=0.48) accuracies for the calibration stage, respectively. Each polynomial consists of $(n+1)^2$ regression coefficients, in which n implies the order of the polynomial. So any increase in polynomial order results in a higher number of regression coefficients. Consequently, the higher number of the regression coefficients will require a better training for polynomials. Results of the other investigations (e.g. Carlson 2007 and Mekonnen 2009) show that the higher order the polynomial, the better accuracy of soil moisture prediction, which also consistent with this study. The best performance for the validation stage ($RMSE$=0.024 cm³cm⁻³, ER=15.85%, and R^2_{adj}=0.60) was also for the 4th order polynomial. However, results of the 1st, 2nd, and 3rd orders polynomials showed that measured soil moisture had the best correlation with the 3rd order polynomial prediction (R^2_{adj}=0.59 *vs*. R^2_{adj}=0.02 and R^2_{adj}=0.37), while the $RMSE$ and ER criterions had the best agreement with the 2nd ($RMSE$=0.026 cm³cm⁻³ and ER=16.96%) and 1st (with $RMSE$=0.034 cm³cm⁻³ and ER=22.53%) order polynomials, with the worst results was for the 3rd order

polynomial prediction (with $RMSE$=0.036 cm³cm⁻³ and ER=24%). Consequently, the 4th order polynomial is proposed for further investigation in the region. The regression coefficients of the 4th order polynomial adopted from the calibration stage are reported in Table 3. The simulated soil moisture maps using the 4th order polynomial are also demonstrated in Figure 6 for both calibration and validation stages. Cross correlation of the measured and simulated soil moistures using the 4th order of polynomial for both calibration and validation stages are depicted in Figure 7, showing a satisfying correlation (calibration R^2=0.840 and validation R^2=0.829) with measured data.

Although, the range of the applied data in this research is restricted (one small catchment and 2 sampling days), the results are encouraging. Gillies *et al.* (1997) estimated soil moisture using *TM* method and multispectral measurements with standard errors of 16 per cent compared to measured soil moisture. Wang *et al.* (2007) also executed a 2nd order polynomial of the *TM* method to estimate soil moisture with a wide range of data (using 93 ground stations data) in eastern China, reporting an R^2 greater than 0.6 between measured and estimated soil moistures for 82 out of 93 ground stations and greater than 0.7 for 71 out of 93 ground stations. Mekonnen (2009) also applied a 3rd order polynomial of the *TM* method in northwest Ethiopia using a wide range data from 9 different days of ground measurement, with an R^2 greater than 0.7 and $RMSE$ of 0.045.

The key advantages of the *TM* method, although, are its independence to surface roughness and applicability to pixels with $NDVI > 0.4$, which is contrary to others microwave remote sensing techniques (Mekonnen 2009), it is expected that applying a wide range of ground measurement to train the polynomials will result in a better prediction of soil moisture. Carlson (2007) confirmed that the most severe limitation of the *TM* method is requiring a flat surface and a large number of pixels over an area with a wide range of soil wetness and fractional vegetation cover.

<div align="center">Table 2. The results of polynomial evaluation for both calibration and validation stages</div>

Order of polynomial	Training				Validation			
	R^2	R^2_{adj}	RMSE (cm^3cm^{-3})	ER (%)	R^2	R^2_{adj}	RMSE (cm^3cm^{-3})	ER (%)
1st order	0.530	0.483	0.022	13.00	0.112	0.023	0.034	22.53
2nd order	0.637	0.544	0.021	12.22	0.501	0.373	0.026	16.96
3rd order	0.761	0.625	0.019	11.07	0.741	0.593	0.036	24.00
4th order	0.840	0.630	0.019	11.00	0.829	0.604	0.024	15.85

Table 3. Regression coefficients (a_{ij}) of the 4th order polynomial, where i and j imply the power of the NDVI* and LST* in Equation (3), respectively

		i				
		0	1	2	3	4
	0	0.1226	0.8685	-5.1687	8.4222	0.1450
	1	-0.0156	-0.7725	0.0323	-11.2971	1.1789
j	2	0.0025	8.0978	-0.0005	-0.3710	0.9904
	3	-2.1639	-2.3652	0.4073	2.5841	-0.4100
	4	0.1665	0.3341	0.0886	-0.0724	-0.5460
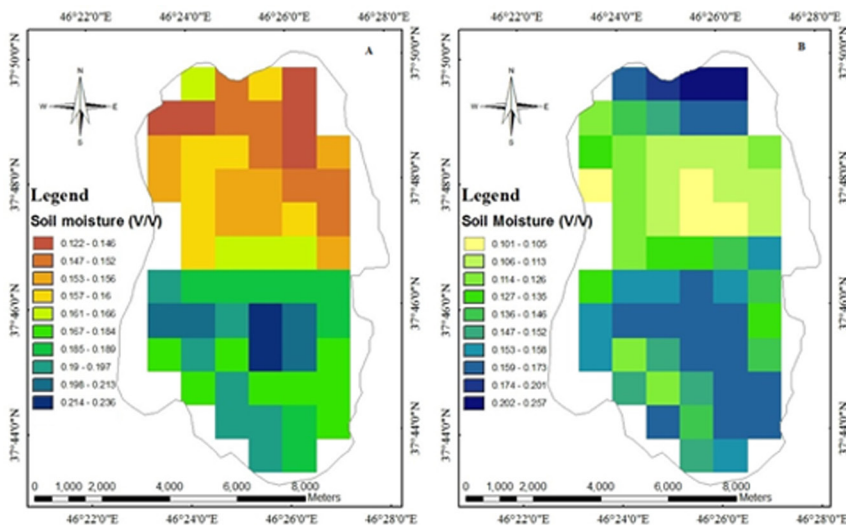
Figure 6. Simulated soil moisture maps by 4th order polynomial for calibration (9-Jun-2012, A) and validation (15-Jun-2012, B) stages
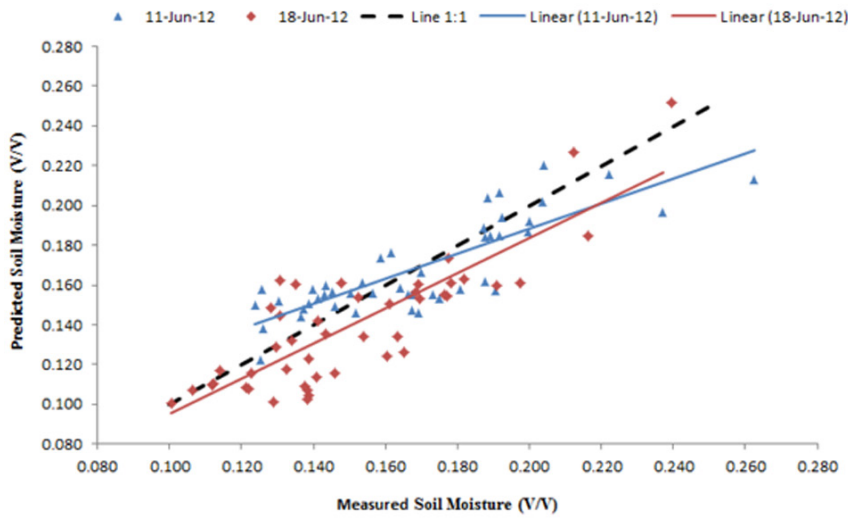
Figure 7. Cross correlation of measured and simulated soil moistures using 4th order polynomial for calibration (9-Jun-2012) and validation (15-Jun-2012) stages

4.3. Terrain effects evaluation on polynomials

Since the topography of the study area is irregular and rough, terrain effects on simulated soil moisture were evaluated. Potential surface temperature was used to correct the topographic effects on simulated soil moisture. The evaluation results of constructed polynomials among soil moisture, *NDVI**, and *T** are reported in Table 4. Although applying potential temperature T instead of LST resulted in a better validation of 3rd order polynomial

(*RMSE* of 0.033 *vs.* 0.036 cm³cm⁻³ and *ER* of 21.7 *vs.* 24.0 %), the other polynomials (1st, 2nd, and 4th orders) showed no sensitivity to the substitution of *LST* by potential temperature. Contrary to the results of this paper, Mekonnen (2009) showed that the elevation correction resulted in better prediction of the soil moisture. This is possibly due to small size (≈ 80 km2) and reduced elevation variation (1200 m) of the study area used here in comparison to his study area (≈ 1768 km2 and 1900 m).

Table 4. The results of polynomials evaluation after elevation correction on LST using Equation (4)

Order of polynomial	Training				Validation			
	R^2	R^2_{adj}	RMSE (cm³cm⁻³)	ER (%)	R^2	R^2_{adj}	RMSE (cm³cm⁻³)	ER (%)
1st order	0.530	0.483	0.022	13.00	0.112	0.023	0.034	22.53
2nd order	0.637	0.544	0.021	12.22	0.501	0.373	0.026	16.95
3rd order	0.761	0.625	0.019	11.07	0.733	0.581	0.033	21.72
4th order	0.840	0.630	0.019	11.00	0.829	0.605	0.024	15.86

5. Conclusion

The 4th order polynomial of the *TM* method using *MODIS* satellite images was shown to predict the soil moisture with R^2_{adj}=0.63, *RMSE* = 0.019 cm³cm⁻³, and *ER* = 11% for calibration; R^2_{adj}=0.60, *RMSE* = 0.024 cm³cm⁻³, and *ER* = 16% for validation. Applying potential temperature *T* instead of *LST* to correct for the terrain effects on the *TM* method performance showed no improvement on the method's efficiency. The good results obtained from the current research suggest that the method warrants evaluation at larger scale, with more field sampling data across a wider range of conditions.

References

Ahmad, S., Kalra, A., Stephen, H. 2010. Estimating soil moisture using remote sensing data: A machine learning approach. Advances in Water Resources. 33, 69–80.

Carlson, T. 2007. An overview of the triangle method for estimating surface evapotranspiration and soil moisture from satellite imagery," Sensors **7**, 1612-1629.

Carlson, T.N., Gillies, R.R., Perry, E. 1994. A method to make use of thermal infrared temperature and NDVI measurement to infer surface soil water content and fractional vegetation cover," Remote sensing Reviews. 9, 161-173.

Carlson, T.N., Gillies, R.R., Schmugge, T.J. 1995. An interpretation of methodologies for indirect measurement of soil-water content. Agricultural and Forest Meteorology. **77**, 191-205.

Castro, M., Parra, J.C., Morales, L.J., Salas, C. 2014. Establishment of empirical relations between fuel moisture content and the normalized difference vegetation index. Journal of Soil Science and Plant Nutrition. 14 (3), 670-675.

Chauhan, N.S., Miller, S., Ardanuy, P. 2003. Space-borne soil moisture estimation at high resolution: a microwave-optical/IR synergistic approach. International Journal of Remote Sensing. 24, 4599-4622.

Curran, P.J. 1985. Principles of Remote Sensing. Longman Scientific and Technical, UK, 282.

Das, N.N., Mohanty, B.P., Cosh, M.H., Jackson, T.J. 2008. Modeling and assimilation of root zone soil moisture using remote sensing observations in Walnut Gulch Watershed during SMEX04. Remote Sensing of Environmental. 112, 415–29.

Davenport, I.J., Fernandez-Galvez, J., Gurney, R.J. 2005. A sensitivity analysis of soil moisture retrieval from the Tau-Omega microwave emission model. IEEE Transactions on Geoscience and Remote Sensing. 43, 1304–1316.

Engman, E.T. 1991. Applications of microwave remote sensing of soil moisture for water resources and agriculture. Remote Sensing of Environment. 35, 213-226.

Friedl, M.A., Davis, F.W. 1994. Sources of variation in radiometric surface temperature over a tall-grass prairie. Remote Sensing of Environment. 48, 1–17.

Gillies, R.R., Carlson, T.N. 1995. Thermal Remote Sensing of Surface Soil Water Content with Partial Vegetation Cover for Incorporation into Climate Models. Journal of Applied Meteorology. 34, 745-756.

Gillies, R.R., Carlson, T.N., Cui, J., Kustas, W.P., Humes, K.S. 1997. A verification of the 'triangle' method for obtaining surface soil water content and energy fluxes from remote measurements of the Normalized Difference Vegetation Index (NDVI) and surface radiant temperature. International Journal of Remote Sensing. 18, 3145-3166.

Guo, Z., Dirmeyer, P.A., Koster, R.D. et al. 2005. GLACE: the global land–atmosphere coupling experiment. Part II: analysis. American Meteorological Society. 7, 611-625.

Jiang, L., Islam, **S. 1999.** A methodology for estimation of surface evapotranspiration over large areas using remote sensing observations. Geophysical Research Letters. 26, 2773-2776.

Jiang, L., Islam, S. 2001. Estimation of surface evaporation map over southern Great Plains using remote sensing data. Water Resources Research. 37, 329-340.

Jiang, L., Islam, S. 2003. An Inter-comparison of Regional Latent Heat Flux Estimation using Remote Sensing Data. International Journal of Remote Sensing. 24, 2221-2236.

Lambin, E.G., Ehrlich, D. 1996. The Surface Temperature-vegetation Index Space for Land Cover and Land-cover Change Analysis. International Journal of Remote Sensing. 17, 463-487.

Mekonnen, D.F. 2009. Satellite remote sensing for soil moisture estimation: Gumara catchment, Ethiopia. Master Science Thesis, International Institute for Geo-information Science and Earth observation, The Netherland.

Owen, T.W., Carlson, T.N., Gillies, R.R. 1998. An assessment of satellite remotely-sensed land cover parameters in quantitatively describing the climatic effect of urbanization. International Journal of Remote Sensing. 19, 1663-1681.

Price, J.C. 1990. Using spatial context in satellite data to infer regional scale evapotranspiration. IEEE Transactions on Geoscience and Remote Sensing. 28, 940-948.

Rahmati, M. 2014. Estimating soil infiltration rate by remote sensing and its using in LISEM model for Lighvan watershed erosion prediction. Thesis for PhD, University of Tabriz, Tabriz, Iran.

Schmugge, T.J. 1978. Remote sensing of surface soil moisture. Journal of Applied Meteorology. 17, 1549–1557.

Serrano, M.H.L.R. 2010. Satellite Remote Sensing of Soil Moisture. Master Science Thesis, Department of Meteorology, University of Reading, England.

Shi, J., Wang, A., Hsu, Y., O'Neill, P.E., Engman, E.T. 1997. Estimation of bare surface soil moisture and surface roughness parameter using L-band SAR image data. IEEE Transactions on Geoscience and Remote Sensing. 35, 1254–66.

Van doninck, J., Peters, J., De Baets, B., De Clercq, E.M., Ducheyne, E., Verhoest, N.E.C. 2011. The potential of multitemporal Aqua and Terra MODIS apparent thermal inertia as a soil moisture indicator. International Journal of Applied Earth Observation and Geoinformation. 13, 934–941.

Wang, L., Qu, J.J. 2009. Satellite remote sensing applications for surface soil moisture monitoring: A review. Frontiers of Earth Science in China. 3, 237-247.

Wang, L., Qu, J. J., Zhang, S., Hao, X., Dasgupta, S. 2007. Soil moisture estmiation using MODIS and ground measurments in eastern China. International Journal of Remote Sensing. 28, 1413-1418.

Wen, J., Su, Z., Ma, Y. 2003. Determination of land surface temperature and soil moisture from tropical rainfall measuring mission/microwave imager remote sensing data. Journal of Geophysical Research. 108, 805–26.

Wood, E.F., Lettenmaier, D.P., Zartarian, V.G. 1992. A land-surface hydrology parameterization with subgrid variability for general circulation models. Journal of Geophysical Research. 97, 2717-2728.